High affinity modified ACE2 receptors prevent SARS-CoV-2 infection

Yusuke Higuchi[1,8], Tatsuya Suzuki[2,8], Takao Arimori[3,8], Nariko Ikemura[1,8], Yuhei Kirita[4], Eriko Ohgitani[5], Osam Mazda[5], Daisuke Motooka[6], Shota Nakamura[6], Yoshiharu Matsuura[7], Satoaki Matoba[1], Toru Okamoto[2]*, Junichi Takagi[3]*, Atsushi Hoshino[1]*

[1] Department of Cardiovascular Medicine, Graduate School of Medical Science, Kyoto Prefectural University of Medicine, Kyoto, Japan.
[2] Institute for Advanced Co-Creation Studies, Research Institute for Microbial Diseases, Osaka University, Osaka, Japan.
[3] Laboratory of Protein Synthesis and Expression, Institute for Protein Research, Osaka University, Osaka, Japan.
[4] Department of Nephrology, Graduate School of Medical Science, Kyoto Prefectural University of Medicine, Kyoto, Japan.
[5] Department of Immunology, Graduate School of Medical Science, Kyoto Prefectural University of Medicine, Kyoto, Japan.
[6] Department of Infection Metagenomics, Research Institute for Microbial Diseases, Osaka University, Osaka, Japan.
[7] Department of Molecular Virology, Research Institute for Microbial Diseases, Osaka University, Osaka, Japan.
[8] These authors contributed equally
*Correspondence: a-hoshi@koto.kpu-m.ac.jp (A.H.), takagi@protein.osaka-u.ac.jp (J.T.), toru@biken.osaka-u.ac.jp (T.O.)

ABSTRACT

The SARS-CoV-2 spike protein binds to the human angiotensin-converting enzyme 2 (ACE2) receptor via receptor binding domain (RBD) to enter into the cell. Inhibiting this interaction is a main approach to block SARS-CoV-2 infection and it is required to have high affinity to RBD independently of viral mutation for effective protection. To this end, we engineered ACE2 to enhance the affinity with directed evolution in human cells. Three cycles of random mutation and cell sorting achieved more than 100-fold higher affinity to RBD than wild-type ACE2. The extracellular domain of modified ACE2 fused to the Fc region of the human immunoglobulin IgG1 had stable structure and neutralized SARS-CoV-2 pseudotyped lentivirus and authentic virus with more than 100-fold lower concentration than wild-type. Engineering ACE2 decoy receptors with directed evolution is a promising approach to develop a SARS-CoV-2 neutralizing drug that has affinity comparable to monoclonal antibodies yet displaying resistance to escape mutations of virus.

INTRODUCTION

Coronavirus disease 2019 (COVID-19) has spread across the world as a tremendous pandemic and presented an unprecedented challenge to human society. The causative agent of COVID-19, SARS-CoV-2 is a single-stranded positive-strand RNA virus that belongs to lineage B, clade 1 of the betacoronavirus genus[1-3]. The virus binds to host cells through its trimeric spike glycoprotein composed of two subunits; S1 is responsible for receptor binding and S2 for membrane fusion[4]. Angiotensin-converting enzyme 2 (ACE2) is lineage B clade 1 specific receptor including SARS-CoV-2 [3]. The receptor binding domain (RBD) of S1 subunit directly binds ACE2 with high affinity, therefore, it is the most important targeting site to inhibit viral infection. In fact, the RBD is the common binding site of effective neutralizing antibodies identified from convalescent patients [5-7].

RNA viruses such as SARS-CoV-2 have high mutation rates [8], which are correlated with high evolvability including the acquisition of anti-viral drug resistance. Neutralizing antibodies are one of the promising approaches to combat COVID-19. Accumulating evidence demonstrated that monoclonal antibodies isolated from convalescent COVID-19 patients have high potency in neutralizing viruses. However, mutations in the spike gene can lead to the SARS-CoV-2 adaptation to such neutralizing antibodies. In the replicating SARS-CoV-2 pseudovirus culture experiment, escape mutation was observed against monoclonal antibody as early as in the first passage [9] and evasion was seen even against the polyclonal convalescent plasma [10]. Notably, some mutations identified in *in vitro* replicating culture experiment are present in natural population according to the database[10], indicating that selection and expansion of escape mutants can occur naturally in the therapeutic use of monoclonal antibodies.

Similarly to the anti-RBD antibodies, extracellular domain of ACE2, soluble ACE2 (sACE2), can also be used to neutralize SARS-CoV-2 as a decoy receptor. The therapeutic potency was confirmed using human organoid [10], and now Apeiron Biologics conducts European phase II clinical trial of recombinant sACE2 against COVID-19. In addition, fusing sACE2 to the Fc region of the human IgG1 has been shown to enhance neutralization capacity [11] as well as to improve the pharmacokinetics to the level of IgG in mice[12]. Most importantly, sACE2 has a great advantage over antibodies due to the resistance to the escape mutation. The virus with escape mutation from sACE2 should have limited binding affinity to cell surface native ACE2 receptors, leading to a diminished or eliminated virulence. Unfortunately, many reports, including our current study, have revealed that the binding affinity of wild-type sACE2 to the SARS-CoV-2 spike RBD is much weaker (K_D ~50 nM) than that of clinical grade antibodies [4,11,13-15] . Thus, the therapeutic potential of the wild-type sACE2 as a neutralizing agent against SARS-CoV-2 is uncertain.

Here we conducted protein engineering with human cell-based directed evolution to improve the binding affinity of ACE2 to the spike RBD. Random mutations were introduced in the protease domain containing the interface to the RBD, then full length ACE2 mutant library was expressed in 293T cells and incubated with fluorescence-labelled RBD. High binding population was sorted and underwent DNA extraction, the bulk of which was further induced with random mutations for the next cycle of

selection. Three cycles of screening resulted in an identification of mutant ACE2 clones with more than 100-fold higher binding affinity to the RBD and lower half-maximal inhibitory concentration (IC50) for SARS-CoV-2 pseudotyped lentivirus as well as authentic virus. The present protein engineering system generates a virus-neutralizing drug that has high affinity comparable with antibodies and can resolve the issue of drug resistance caused by escape mutation.

RESULTS

We engineered ACE2 to bind the RBD of the SARS-CoV-2 spike protein with the combination of surface display of mutagenized library and fluorescence-activated cell sorting (FACS) to perform the evolution in 293T human cells. The protease domain (PD) of ACE2 is known to harbor the interface to viral spike protein, located in the top-middle part of ACE2 ectodomain. In this study, ACE2 residues 18-102 and 272-409, referred to as PD1 and PD2, respectively, were mutagenized independently. Synthetic signal sequence and HA tag were appended and restriction sites were introduced in both sides of PD1 and PD2 by optimizing codon (Fig. 1a). We used error-prone PCR to mutagenize the protease domain of ACE2 with an average of about one amino acid mutation per 100 bp, then inserted the fragment into the introduced restriction site by homologous recombination. The reaction sample was transformed to competent cell, generating a library of ~10^5 mutants. Mutant plasmid library was packaged into lentivirus, followed by expression in human 293T cells in less than 0.3 MOI (multiplicity of infection) to yield no more than one mutant ACE2 per cell. Cells were incubated with recombinant RBD of SARS-CoV-2 spike protein fused to superfolder GFP (sfGFP; Fig. 1b). We confirmed the level of bound RBD-sfGFP and surface expression levels of HA-tagged ACE2 with Alexa Fluor 647 in two-dimensional display of flow cytometry. Top 0.05 % cells showing higher binding relative to expression level were harvested from ~5 x 10^7 cells by FACS. To exclude the structurally unstable mutants, cells with preserved signal of surface ACE2 were gated. Genomic DNA was extracted from collected cells and mutagenized again to proceed to the next cycle of screening (Fig. 1c).

Random mutagenesis screening for PD1 was performed 3 times and mutated sequences from top 0.05% population were reconstructed into the backbone plasmid, and expressed in 293T cells individually. One to three hundred clones were validated for the binding capacity to the RBD-sfGFP. As the selection cycle advances, the two-dimensional distribution of library cells in flowcytometry became broader and higher in RBD-binding signal, and individual clone validation identified several mutants with higher binding capacity (Fig.2a). To evaluate the neutralization activity in the form of sACE2, we first generated fusion protein of the soluble extracellular domain of mutagenized ACE2 residues 18-614 and sfGFP (sACE2-sfGFP) and used them to compete with the cell-surface WT ACE2 for the RBD binding. To this end, concentration of each mutant sACE2-sfGFP in the cultured medium from transfected cells was quantitatively standardized with sfGFP signal, serially diluted, preincubated with RBD-sfGFP for 30 min, and then transferred to wild-type ACE2 expressing 293T cells. After 30 min, the RBD-bound cells were analyzed in flowcytometry. Higher neutralization activity against the

RBD was confirmed for the mutants that have accumulated mutations (Fig. 2b, Table. S1).

Second mutagenesis based on the top hit of first screening, 1-19 mutant, was also performed, but the distribution of the library cells did not expand so much, and we could not isolate clones with significantly higher affinity than the bulk of top 0.05% (Fig. S1). We next performed PD2 mutagenesis in both the bulk of top 0.05% and one of the highest mutants of the 3rd library, the clone 3N39. Again, the binding distribution of the PD2 library cells was similar to the basal cells, suggesting the inability of this strategy to further increase the affinity to RBD. A recent study reported, via deep mutational scanning, that several specific mutations in PD2 were enriched in high RBD-binding clones [13]. When we added these mutations in 3N39, it did not improve the capacity of the RBD neutralization further (Fig. S2).

To identify essential mutation(s) in the high affinity ACE2 mutants, each mutation was altered to wild-type in mutant 3N39, 3J113 and 3j320. Mutant 3N39 contains 7 mutations of A25V, K26E, K31N, E35K, N64I, L79F, and N90H. Among them, individual back-mutation of V25, N31, K35, and F79 to wild-type residues resulted in modest to severe reduction of the RBD-neutralization capacity (Fig. 3a), while multiple back mutations of E26, I64, and H90 in various combination did not alter the high activity of the original 3N39 (Fig. 3b), indicating that A25V, K31N, E35K, and L79F was necessary and sufficient components. In the case of mutant 3J113 that is composed of K31M, E35K, Q60R, S70F, L79F, and N90D, similar back mutation experiment revealed that K31M, E35K, and Q60R was essential (Fig. 3c). Simultaneous back mutations of two (F70/F79 and F70/D90) but not three (F70/F79/D90) nonessential residues were tolerated (Fig. 3d), suggesting that L79F and N90D may exert their positive effect on the activity only when they coexist. The third mutant 3J320 has T20I, A25V, H34A, T78R, T92Q, and Q101H. Single and multiple back mutation experiments showed that H34A, T92Q, and Q101H were essential in securing the high inhibitory activity of 3J320 (Figs. 3e, f). These top 3 high affinity mutants exhibited higher RBD-neutralization activity when compared with the same sACE2 scaffold carrying the two high affinity mutation sets reported recently [11,13] (Fig. 3g).

First mutant library was also sorted in the manner of high and low RBD-sfGFP binding signal (Fig. S2a). The affinity value of each mutant was defined as the ratio of high and low read counts. Then, the impact of each amino acid mutation on RBD binding was analyzed as a semi-deep mutational scanning (DMS) (Fig. S2b). This analysis revealed that some mutations such as K31N, E35K, and Q60R in top 3 high affinity mutants had very mild impact in itself. Simple combination of high value mutations, A25V, K26T, Q42L, L79V and T92K, referred to here as the DMS mutant, and its derivatives showed less neutralization activity than top three high affinity mutants, indicating that each mutation works coordinately in high affinity mutants (Fig. 3h).

Next, we characterized the binding affinities of the mutant sACE2s for spike RBD using surface plasmon resonance, where IgG1-Fc fused RBD was immobilized as a ligand and the association and dissociation kinetics of his-tagged sACE2 were determined. The K_D value of wild type sACE2 was 41.4 nM, whereas those of mutants 3J38 and 3N39 were determined to be 6.5 nM and 0.37 nM (Fig. 4a). Analytical size exclusion chromatography (SEC) showed no signs of protein aggregation in the ACE2

mutant samples, confirming that the apparent high affinity was not caused by the avidity effect and the observed K_D values represent genuine 1:1 affinity toward RBD (Fig. S4a). Recombinant soluble ACE2 (rsACE2) was reported to have a fast clearance rate in human blood with a half-life of hours [16,17]. Recently, it was demonstrated that a rsACE2 fused with a Fc fragment show high stability in mice [12] as well as higher neutralization activity toward both pseudotyped and authentic SARS-CoV-2 in cultured cells[11]. We formulated our high affinity mutant sACE2s as Fc fusion (sACE2-Fc) and found that the purified proteins were folded well and devoid of aggregation, showing solution behavior indistinguishable from wild type protein (Fig. S4b). To evaluate their efficacy in neutralizing SARS-CoV-2 infections, affinity-enhanced sACE2-Fc mutants were assayed for viral neutralization against pseudotyped lentivirus and authentic SARS-CoV-2. The IC50 values of wild-type, 3J38, and 3N39 for pseudovirus neutralization in ACE2-expressing 293T cells were 65.2, 8.9, and 0.43 μg/ml, respectively. In the same way, 3N39 neutralized pseudovirus very efficiently with an IC50 value more than 100 times lower than the wild-type in TMPRSS2-expressing VeroE6 cells, (Fig. 4b). Most importantly, when the neutralization potential against the authentic SARS-CoV-2 in TMPRSS2-expressing VeroE6 cells was evaluated, wild-type sACE2-Fc showed no efficiency even at 100 μg/ml, whereas 3N39 sACE2-Fc demonstrated significant neutralizing effect in 6.3 μg/ml (Fig. 4c).

DISCUSSION

SARS-CoV-2 neutralization is one of the preventative or therapeutic approaches against COVID-19. Monoclonal antibodies have become one of the common drug modalities, especially as therapeutics against autoimmune diseases and cancer. As virus-neutralizing antibodies, Palivizumab is clinically used to prevent hospitalization from respiratory syncytial virus infection in high-risk infants[18], and cocktail of monoclonal antibodies has been shown to reduce mortality from Ebola virus disease[19]. Engineered recombinant decoy receptor drugs are also developed to neutralize various cytokines including vascular endothelial growth factor, tumor necrosis factor alpha, and CTLA-4 and approved for orbital vascular diseases and rheumatoid arthritis. Recombinant sACE2 or sACE2-Fc fusion protein has potency to neutralize SARS-CoV-2[12,20], however its modest binding affinity requires higher dose than monoclonal antibody.

We developed the screening system based on the cycle of random mutation and sorting of high affinity population in 293T cells followed by validation of neutralizing activity in a soluble form. In this screening, an additional random mutation was induced in the bulk of sorted mutants, which worked better than mutagenesis in the top mutant. Engineering of decoy receptors with improved affinity was previously reported for cancer-related molecules and ACE2[11,21,22]. They used yeast display system to perform directed evolution. Large scale library (~10^7 mutants) was prepared and high affinity mutants were identified by repeating sorting from initial library. Fast growth rate of yeast is suitable for library screening involving repeated sorting and propagation. We on the other hand employed human cells for the display purpose. Since post-translational modification can modulate protein binding affinity,

human cell-based screening is better to understand the impact of ACE2 variants on viral affinity and also to proceed biologics development. Repeating mutagenesis after cell sorting without propagation enabled us to conduct screening with relatively small library (~10^5 mutants) and human cells. During the validation, we noticed that high affinity pattern in the flow cytometry assay of full length ACE2 binding RBD-sfGFP did not always correlate with its neutralization activity. Thus, it is evident that experimental validation of each mutation at the level of sACE2 protein was important for efficient identification of high affinity mutants.

Our mutant ACE2s have affinity comparable to typical anti-spike monoclonal antibodies, but they also offer some advantages over antibodies when considered as a drug candidate. Interface of ACE2 to the RBD is larger than that of antibodies, which potentially increases efficacy. Escape mutation to modified ACE2 is likely to result in lower affinity to the native receptor, making such virus much less virulent. SARS-CoV-2 also enters into host cell via endocytosis. SARS-CoV-2 infection is mediated not only by TMPRSS family proteases but by cathepsin L that is catalytically active at pH 3.0–6.5[23]. Some antibodies are susceptible to impaired affinity at lower pH, leading to lower viral neutralization.

High affinity modified ACE2 fused with Fc is the promising strategy to neutralize SARS-CoV-2. The time frame for running one cycle of mutagenesis and sorting was just one week in our system, and we succeeded in developing optimized mutants in a couple of months without depending on patients-derived cells or tissues. Thus, our system can rapidly generate therapeutic candidates against various viral diseases and may be well suited for fighting against future viral pandemics.

METHODS

Cell culture

Lenti-X 293T cells were purchased from Clontech and cultured at 37 ° C with 5% CO_2 in Dulbecco's modified Eagle's medium (DMEM, WAKO) containing 10% fetal bovine serum (Gibco) and penicillin/streptomycin (100 U/ml, Invitrogen). VeroE6/TMPRSS2 cells were a gift from National Institutes of Biomedical Innovation, Health and Nutrition (Japan) and cultured at 37 ° C with 5% CO_2 in DMEM (WAKO) containing 5% fetal bovine serum (Gibco) and penicillin/streptomycin (100 U/ml, Invitrogen). All the cell lines were routinely tested negative for mycoplasma contamination.

Plasmids

The mature polypeptide (a.a. 18-805) of human ACE2 (GenBank NM_021804.1) was cloned into the KpnI-XhoI sites of pcDNA4TO (Invitrogen) or the XbaI-SalI sites of pLenti puro with a N-terminal synthetic leader (MWWRLWWLLLLLLLLWPMVWA)[24], HA-tag, and linker (GSGG). Some codon optimizations were introduced to generate BamHI and SacII and destroy original BamHI and SacII restriction sites. Soluble ACE2 (a.a. 1-615) fused to superfolder GFP (sfGFP) with a linker

(GSGGSGSGGS) was placed between the BamHI-XhoI sites of the former plasmid. Equivalent sACE2 constructs were cloned with TEV protease cleavage site and 8 histidine tag or the Fc region of IgG1 into the KpnI-BstBI sites of pcDNA3.1-MycHis (Invitrogen) or the HindIII-BamHI sites of p3xFLAG-CMV-14 (Invitrogen). A codon-optimized RBD (a.a. 333-529) of SARS-CoV-2 Spike fused to sfGFP was obtained from addgeen #141184 [13] and cloned into the KpnI-XhoI sites of pcDNA4TO (Invitrogen) with a N-terminal synthetic leader, HA-tag, and linker (GSGG).

Library preparation

Error-prone PCR was performed in ACE2 residues 18-102 and 272-409 independently using GeneMorph II Random Mutagenesis Kit (Agilent). A 0.1 ng of plasmid was used as a PCR template and generated mutations with an average of about one mutation per 100 bp in 35- cycle reaction. The plenti ACE2 vector was digested with BamBI or MfeI-SacII (NEB) for ACE2 residues 18-102 or 272-409, respectively with alkaline phosphatase (Fermentas) at 37° C for 2 hours and gel-purified on a Gel and PCR Clean-up kit (TAKARA). A 160 μl NEBuilder ligation reaction (NEB) was performed using 5 ng of the gel-purified inserts and 10 ng of the vector, then purified on a Gel and PCR Clean-up kit (TAKARA) and eluted by a 20 μl of distilled water. From the ligation, 400 μg (~8 μl) of the purified reaction was transformed into 100 ul of electrocompetent cells (Lucigen) and expanded according to the manufacturer's protocol with 1500V electroporation by ECM 399 (BTX). A 1,000-fold dilution of the full transformation was plated to estimate the scale of mutant library.

Virus production

Ten-centimetre plates of 70% confluent Lenti-X 293T (Clontech) cells were transfected with 9 μg of the plasmid library, 6 μg of psPAX2 vector and 3 μg pMD2.G using Fugene HD (Promega) according to the manufacturer's instructions. Supernatant was collected after 48 h and then spun for 10 min at 4 ° C at 3,000 rpm and then filtered with a 0.45 μm low protein-binding filter (SFCA), and frozen at –80 ° C. The titre of the virus was determined by using 293T cells followed by puromycin selection.

Library screening

The mutant library was transduced into 293T cells via spinfection. To find optimal virus volumes for achieving a multiplicity of infection (MOI) of 0.1–0.3, each library virus was tested by spinfecting $5x10^5$ cells with several different volumes of virus in the 6-well plate. Each well received a different titrated virus amount (usually between 50 and 500 μl) along with a no-transduction control and infected cell rate was determined by anti-HA Alexa 594. Then, four 6-well plates, 1.2 x 10^7 cells were centrifuged at 1,000 g for 1.5 hours at 37° C.

Cells were sorted using a SH800 (SONY) 24 hr after spinfection. Approximately $5x10^7$ induced library cells were resuspended with complete medium and incubated for 30 minutes at 4° C with a 1/40~1/160 dilution of medium containing RBD-sfGFP and a 1/4000 dilution of anti-HA Alexa 647

(clone TANA2, MBL). Cells were directly sorted on SH800 (SONY). The top 0.5 % of cells were sorted and their genomic DNA was extracted by NucleoSpin Tissue (TAKARA). Mutated ACE2 fragment was cloned into pcDNA4TO ACE2 for individual validation and also introduced random mutations again with error-prone PCR for further screening.

For a semi-deep mutational scanning of ACE2 residues 18-102, 30 % of HA positive cells with the highest and 30% with the lowest GFP fluorescence were also collected in 1st mutated library (Fig. S3a) and their genomic DNA was extracted by NucleoSpin Tissue (TAKARA). ACE2 residues 18-102 plasmid sequence was amplified with primers containing adaptor and barcode sequence to perform deep sequencing on the Illumina MiSeq platform using 300nt paired-end protocol. Data were analyzed as follows; high and low gating read count of each mutant was normalized with total counts and log10 ratio of high/low was defined as affinity value. Then, each amino acid mutation-containing mutant affinity values were aggregated.

.

Flow Cytometry Analysis

The pcDNA4TO HA-ACE plasmid was transfected into 293T cells (500 ng DNA per ml of culture at 5 × 105 / ml) using Fugene HA (Promega). Cells were analyzed by flow cytometry 24 h post-transfection. To analyze binding of RBD-sfGFP to full length HA-ACE2, cells were washed, trypsinized, and resuspended with complete medium, then incubated for 30 minutes at 4° C with a 1/40~1/160 dilution of medium containing RBD-sfGFP and a 1/4000 dilution of anti-HA Alexa 594 (clone TANA2, MBL). Cells were directly analyzed on Attune NxT Flow Cytometer (Invitrogen).

To analyze binding of sACE2-sfGFP to RBD-sfGFP, a serial dilution of medium containing sACE2-sfGFP and a 1/40 dilution medium containing RBD-sfGFP were mixed and incubated for 1 hour at 4° C, then HA-ACE2 expressing 293T cells were resuspended and incubated with the mixture and a 1/1000 dilution of anti-HA Alexa 594 (clone TANA2, MBL) for 30 minutes at 4° C. Cells were directly analyzed on Attune NxT Flow Cytometer (Invitrogen). Data were processed with FlowJo (FlowJo, LLC). Data are biological replicates.

Protein synthesis and purification

sACE2-His, sACE2-Fc, and RBD-Fc were expressed using the Expi293F cell expression system (Thermo Fisher Scientific) according to the manufacturer's protocol. His-tagged and Fc-fused proteins were purified from conditioned media using the Ni-NTA agarose (QIAGEN) and the rProtein A Sepharose Fast Flow (Cytiva), respectively. Fractions containing target proteins were pooled and dialyzed against phosphate buffered saline (PBS).

Kinetic binding measurement using Biacore (SPR)

The binding kinetics of sACE2 (wild-type or mutants) to RBD were analyzed by SPR using a Biacore T200 instrument (Cytiva) in a single-cycle kinetics mode. Anti-human IgG (Fc) antibody was immobilized onto a CM5 sensor chip (Cytiva) using the Human Antibody Capture Kit (Cytiva)

according to the method provided by the manufacturer. The RBD-Fc was captured on the measurement cell via the antibody at a density of ~450 RU, while human IgG1-Fc was captured on the reference cell at a density of ~200 RU. The binding was evaluated by injecting various concentrations of sACE2-His solutions in series using PBS containing 0.05% Tween 20 as a running buffer. The runs were conducted at 25° C employing the following parameters; flow rate of 30 μl/min, contact time of 120 s, and dissociation time of 480 s. After each run, the surface was regenerated by injecting the Regeneration solution contained in the kit for 30 sec. The binding curves of the measurement cell were subtracted with those of the reference cell, and used to derive kinetic binding values. The results were evaluated by using Biacore T200 evaluation software version 4.1.

Analytical Size Exclusion Chromatography (SEC)

Purified sACE2 proteins (20 μg, 100 μl) were loaded on a Superdex 200 Increase 10/300 column (Cytiva) equilibrated with PBS. Apparent molecular weight of each elution peak was calculated by using the standard molecular size marker containing thyroglobulin (670 kDa), ferritin (440 kDa), γ-globulin (158 kDa), ovalbumin (44 kDa), myoglobin (17 kDa) and vitamin B12 (1.35 kDa).

SARS-CoV-2 pseudotyped virus neutralization assay

Pseudotyped reporter virus assays were conducted as previously described [25]. A plasmid coding SARS-CoV-2 Spike was obtained from addgene #145032 [14], and deletion mutant CΔ19 (with 19 amino acids deleted from the C terminus) was cloned into pcDNA4TO (Invitrogen) to enhance virus titer[26]. Spike-pseudovirus with a luciferase reporter gene was prepared by transfecting plasmids (CΔ19, psPAX2, and pLenti firefly) into LentiX-293T cells with Lipofectamine 3000 (Invitrogen). After 48 hours, supernatants were harvested, filtered with a 0.45 μm low protein-binding filter (SFCA), and frozen at –80 ° C. ACE2-expressing 293T cells were seeded at 10,000 cells per well in 96-well plate. Pseudovirus and three-fold dilution series of sACE2-Fc protein were incubated for 1 hour, then this mixture was administered to ACE2-expressing 293T cells. After 1 hour pre-incubation, medium was changed and cellular expression of luciferase reporter indicating viral infection was determined using Dual-Glo™ Luciferase Assay System (Promega) in 48 hours after infection.

SARS-CoV-2 neutralization assay at biosafety level 3.

SARS-CoV-2 strain was isolated at National Institute of Infectious Diseases (NIID). Vero-TMPRSS2 were seeded at 80,000 cells in 24 well plates and incubated for overnight. Then, SARS-CoV-2 was infected at MOI of 0.1 together with sACE2-Fc protein. After 2 hours, culture medium was discarded, washed by PBS and incubated for 22 hours. Culture supernatants were collected and performed plaque assay. The attached cells were washed by PBS and extracted RNA for quantification of viral RNA.

SARS-CoV-2 virus plaque assays

Vero-TMPRSS2 were seeded on 24 well plates (80,000 cells/well) and incubated for overnight. The culture supernatants serially diluted by medium were inoculated and incubated for 2 hours. Culture medium was removed, fresh medium containing 1% methylcellulose (1.5mL) was added, and the culture was further incubated for 3 days. The cells were fixed with 4% Paraformaldehyde Phosphate Buffer Solution (Nacalai Tesque) and plaques were visualized by using a Crystal violet.

Quantitative PCR

Total RNA was isolated using ISOGENE II (NIPPON GENE). cDNA was synthesized using 500 ng of total RNA with a PrimeScript RT reagent Kit (Perfect Real Time) (Takara). Real-time RT-PCR was performed with the SYBR Green PCR Master Mix (Applied Biosystems) using a AriaMx Real-Time PCR system (Agilent). The relative quantitation of target mRNA levels was performed by using the 2-ΔΔCT method. The values were normalized by those of the housekeeping gene, *glyceraldehyde 3-phosphate dehydrogenase* (*GAPDH*). The following primers were used: for GAPDH 5'-TGTAGTTGAGGTCAATGAAGGG -3' and 5'- ACATCGCTCAGACACCATG -3' , for SARS-CoV-2 5'-CCAGGTAACAAACCAACCAACTTTCG-3'and 5'-GGTTACTGCCAGTTGAATCTGAGG-3'.

ACKNOWLEDGEMENTS

We would like to thank Sho Hashimoto, Toshiyuki Nishiji, Tomohiro Hino, and Keiko Tamura-Kawakami for the construction of expression vectors; Yukiko Takemura for production of ACE2 proteins; Tomoya Kitani and Daisuke Ueno for the validation experiment; Shunta Taminishi for NGS sample preparation; Takeshi Yaoi for helpful discussion and support. This work was supported in part by KAKENHI 19H03658 to A.H., Japan Agency for Medical Research and Development (AMED), Platform Project for Supporting Drug Discovery and Life Science Research (Basis for Supporting Innovative Drug Discovery and Life Science Research) under 20am0101075 to J.T. and Research Program on Emerging and Re-emerging Infectious Diseases under JP20fk0108263 to T.O..

REFERENCES

1. Zhou, P., *et al.* A pneumonia outbreak associated with a new coronavirus of probable bat origin. *Nature* **579**, 270-273 (2020).
2. Wu, F., *et al.* A new coronavirus associated with human respiratory disease in China. *Nature* **579**, 265-269 (2020).
3. Letko, M., Marzi, A. & Munster, V. Functional assessment of cell entry and receptor usage for SARS-CoV-2 and other lineage B betacoronaviruses. *Nat Microbiol* **5**, 562-569 (2020).
4. Wrapp, D., *et al.* Cryo-EM structure of the 2019-nCoV spike in the prefusion conformation.

Science **367**, 1260-1263 (2020).

5. Shi, R., *et al.* A human neutralizing antibody targets the receptor-binding site of SARS-CoV-2. *Nature* **584**, 120-124 (2020).
6. Ju, B., *et al.* Human neutralizing antibodies elicited by SARS-CoV-2 infection. *Nature* **584**, 115-119 (2020).
7. Cao, Y., *et al.* Potent Neutralizing Antibodies against SARS-CoV-2 Identified by High-Throughput Single-Cell Sequencing of Convalescent Patients' B Cells. *Cell* **182**, 73-84 e16 (2020).
8. Duffy, S. Why are RNA virus mutation rates so damn high? *PLoS Biol* **16**, e3000003 (2018).
9. Baum, A., *et al.* Antibody cocktail to SARS-CoV-2 spike protein prevents rapid mutational escape seen with individual antibodies. *Science* **369**, 1014-1018 (2020).
10. Weisblum, Y., *et al.* Escape from neutralizing antibodies by SARS-CoV-2 spike protein variants. *bioRxiv* (2020).
11. Glasgow, A., *et al.* Engineered ACE2 receptor traps potently neutralize SARS-CoV-2. *bioRxiv* (2020).
12. Lei, C., *et al.* Neutralization of SARS-CoV-2 spike pseudotyped virus by recombinant ACE2-Ig. *Nat Commun* **11**, 2070 (2020).
13. Chan, K.K., *et al.* Engineering human ACE2 to optimize binding to the spike protein of SARS coronavirus 2. *Science* (2020).
14. Shang, J., *et al.* Structural basis of receptor recognition by SARS-CoV-2. *Nature* **581**, 221-224 (2020).
15. Lan, J., *et al.* Structure of the SARS-CoV-2 spike receptor-binding domain bound to the ACE2 receptor. *Nature* **581**, 215-220 (2020).
16. Wysocki, J., *et al.* Targeting the degradation of angiotensin II with recombinant angiotensin-converting enzyme 2: prevention of angiotensin II-dependent hypertension. *Hypertension* **55**, 90-98 (2010).
17. Haschke, M., *et al.* Pharmacokinetics and pharmacodynamics of recombinant human angiotensin-converting enzyme 2 in healthy human subjects. *Clin Pharmacokinet* **52**, 783-792 (2013).
18. Palivizumab, a humanized respiratory syncytial virus monoclonal antibody, reduces hospitalization from respiratory syncytial virus infection in high-risk infants. The IMpact-RSV Study Group. *Pediatrics* **102**, 531-537 (1998).
19. Mulangu, S., *et al.* A Randomized, Controlled Trial of Ebola Virus Disease Therapeutics. *N Engl J Med* **381**, 2293-2303 (2019).
20. Monteil, V., *et al.* Inhibition of SARS-CoV-2 Infections in Engineered Human Tissues Using Clinical-Grade Soluble Human ACE2. *Cell* **181**, 905-913 e907 (2020).
21. Kariolis, M.S., *et al.* An engineered Axl 'decoy receptor' effectively silences the Gas6-Axl signaling axis. *Nat Chem Biol* **10**, 977-983 (2014).
22. Kim, J.W., *et al.* Antitumor activity of an engineered decoy receptor targeting CLCF1-CNTFR signaling in lung adenocarcinoma. *Nat Med* **25**, 1783-1795 (2019).

23. Wei, J., *et al.* Genome-wide CRISPR screen reveals host genes that regulate SARS-CoV-2 infection. *bioRxiv* (2020).

24. Barash, S., Wang, W. & Shi, Y. Human secretory signal peptide description by hidden Markov model and generation of a strong artificial signal peptide for secreted protein expression. *Biochem Biophys Res Commun* **294**, 835-842 (2002).

25. Crawford, K.H.D., *et al.* Protocol and Reagents for Pseudotyping Lentiviral Particles with SARS-CoV-2 Spike Protein for Neutralization Assays. *Viruses* **12**(2020).

26. Giroglou, T., *et al.* Retroviral vectors pseudotyped with severe acute respiratory syndrome coronavirus S protein. *J Virol* **78**, 9007-9015 (2004).

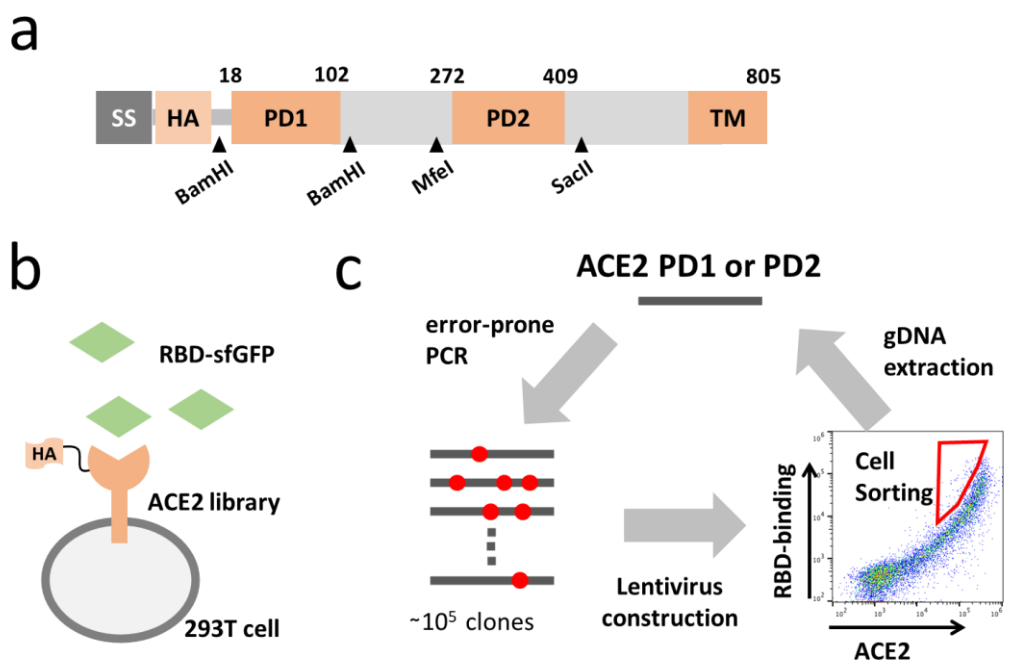

Figure 1. Directed evolution of ACE2. (**a**) Full length ACE2 was optimized to fit screening. Synthetic signal sequence and HA tag were fused to mature ACE2 and restriction sites were introduced by optimizing codon optimization for the mutated fragment replacement. (**b**) ACE2 mutant library was expressed in 293T cell and incubated with the RBD of SARS-CoV-2 fused to superfolder GFP (sfGFP). (**c**) Error-prone PCR amplification of ACE2 protease domain induced random mutations in the rate of one mutation per 100bp and generated a library of ~10^5 mutants. Mutant library-transduced cells were incubated with the RBD-sfGFP. Top 0.05 % population with high level of bound RBD-sfGFP relative to ACE2 expression was sorted and underwent DNA extraction, followed by next cycle mutagenesis.

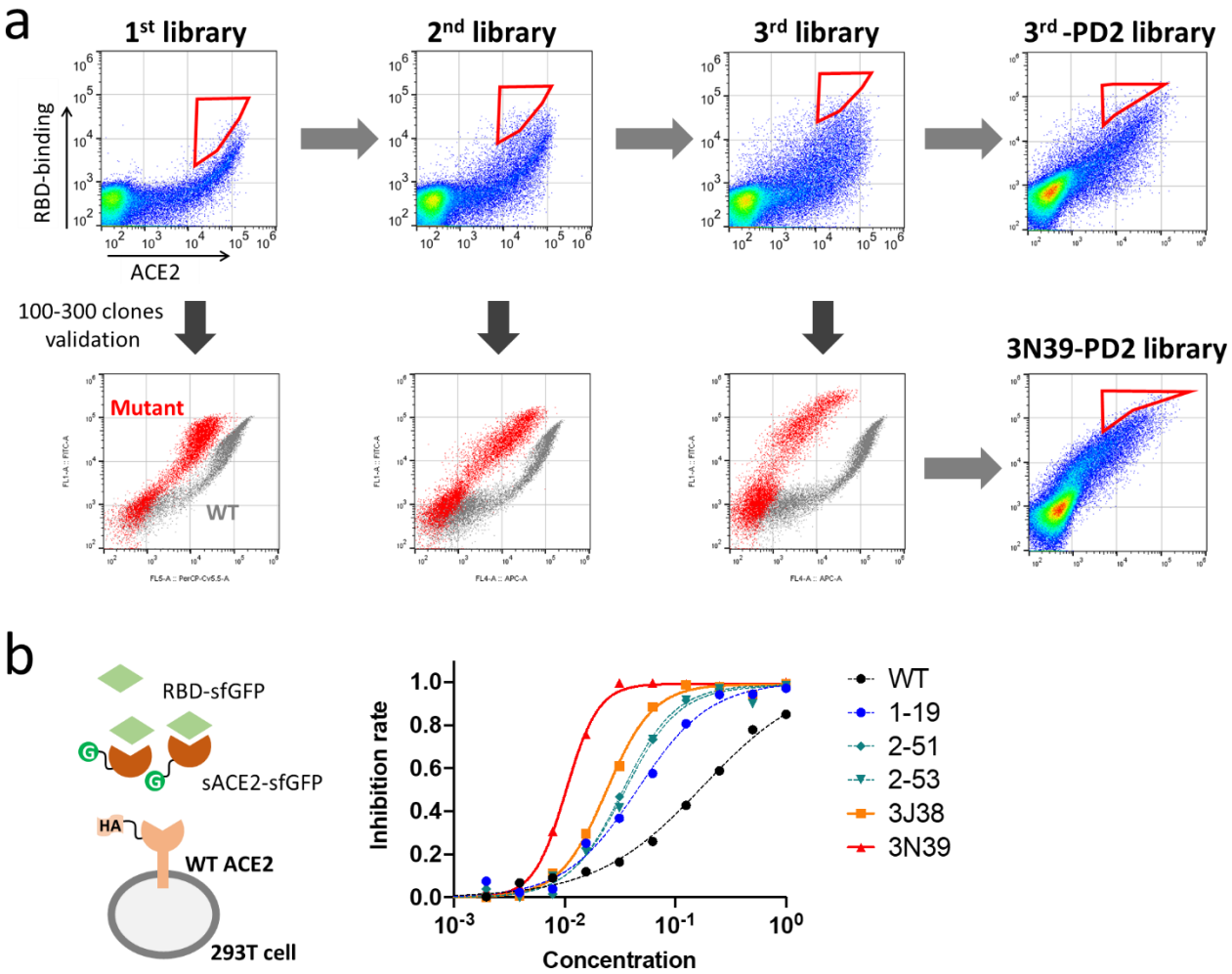

Figure 2. High affinity ACE2 according to the repeat of mutagenesis. (**a**) PD1 mutagenesis and high affinity selection were performed 3 times and followed by PD2 random mutation. Top 0.05% population were harvested and reconstructed into the backbone plasmid. Individual mutant verified higher binding to the RBD in parallel with the number of mutagenesis. (**b**) Neutralization activity against the RBD was evaluated with sACE2-sfGFP and the RBD-sfGFP. Serial dilution of sACE2-sfGFP was analyzed with the 50-fold diluted RBD-sfGFP in flowcytometry. The experiments were independently performed twice and similar results were obtained. One representative data were shown.

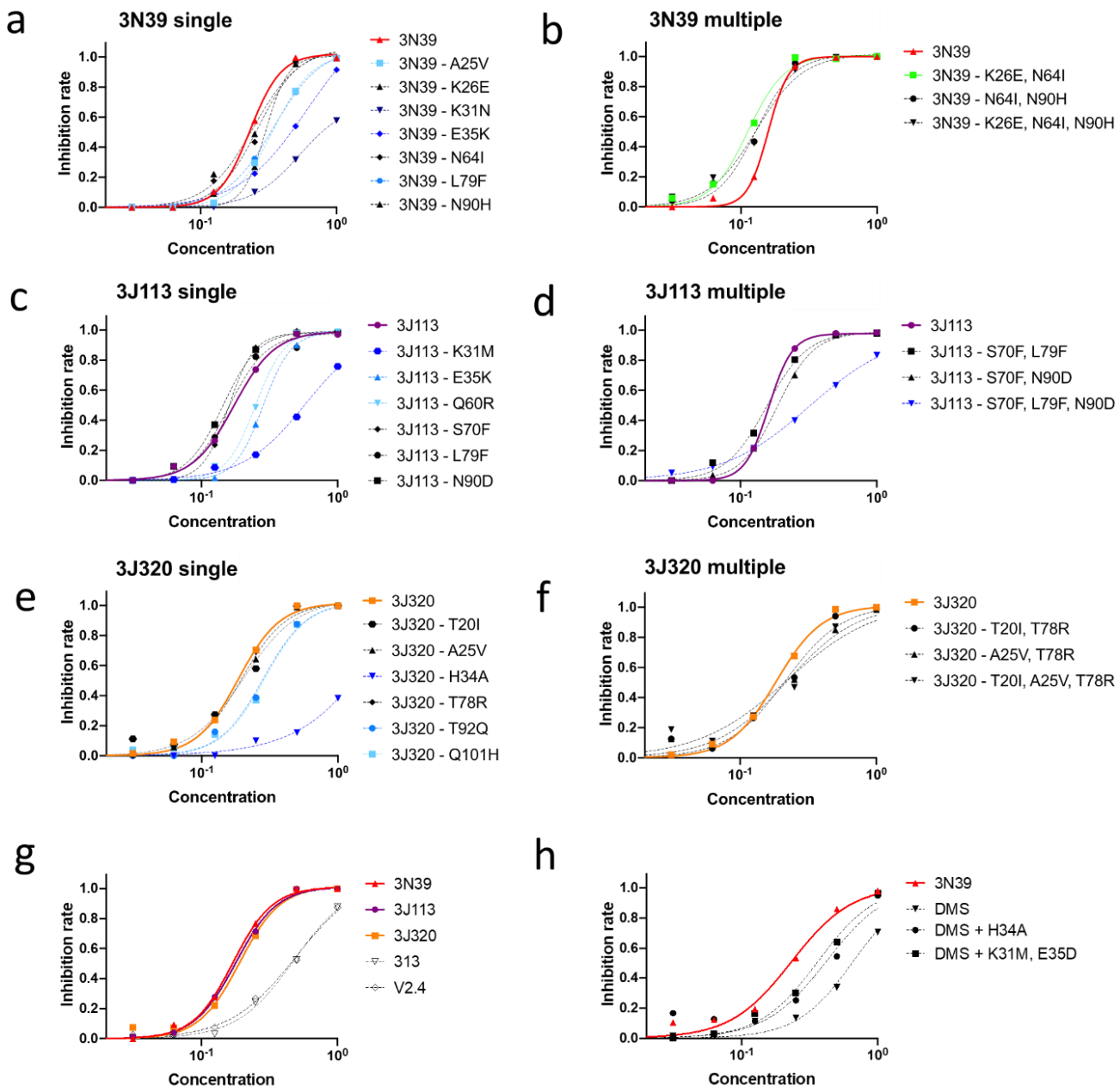

Figure 3. The contribution of each mutation in high affinity mutants. Serial dilution of sACE2-sfGFP was analyzed with 20-fold dilution of the RBD-sfGFP in flowcytometry. (**a-f**) Each mutation was recovered to wild-type and then analyzed the alteration of neutralization capacity individually in 3N39 (a), 3J113 (c), and 3J320 (e) and also in the combination of non-essential mutations in 3N39 (b), 3J113 (d), and 3J320 (f). (**g**) High affinity mutants were compared the RBD-neutralization capacity with mutant 313 in Wells' paper and v2.4 mutant in Procko's paper. (**h**) The DMS mutant from semi-deep mutational scanning and its derivatives were compared with 3N39 mutant. The experiments were independently performed twice and similar results were obtained. One representative data were shown.

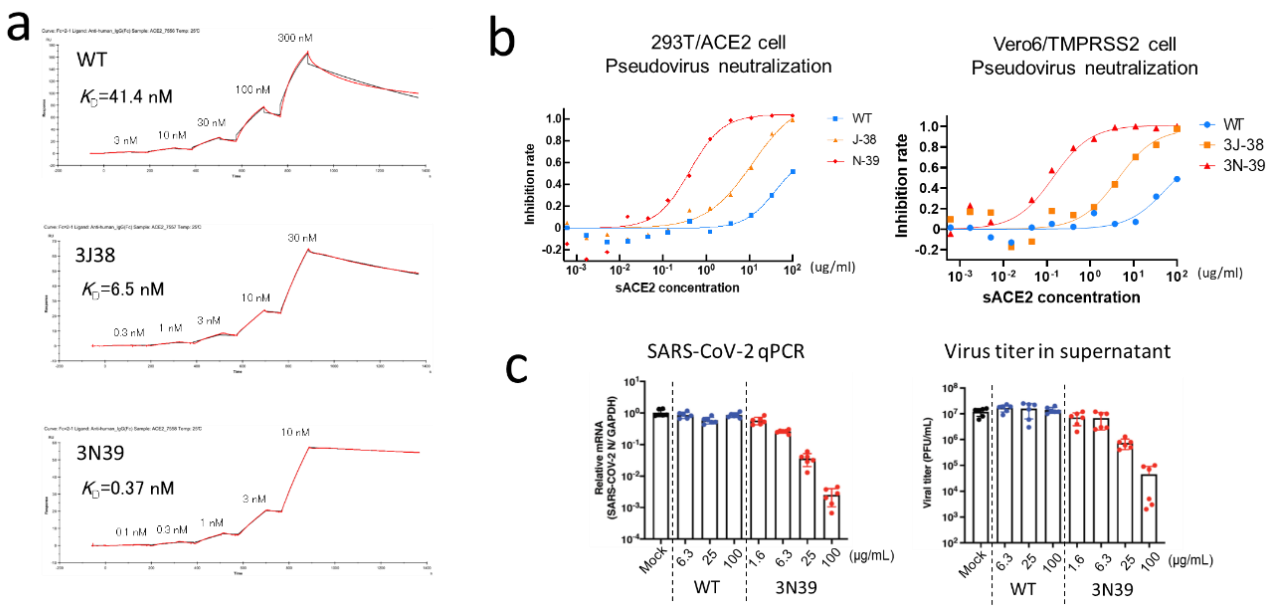

Figure 4. High affinity modified sACE2-Fc neutralized SARS-CoV-2. The contribution of each mutation in high affinity mutants. (**a**) Kinetic analysis of sACE2-His binding to RBD-Fc was analyzed by surface plasmon resonance (SPR). (**b**) Neutralization potency of sACE2-Fc against SARS-CoV-2 pseudotyped lentivirus was measured in ACE2 expressing 293T cells (left) and TMPRSS2 expressing Vero6E cells (right). The experiments were independently performed twice and similar results were obtained. One representative data were shown. (**c**) Neutralization potency to authentic SARS-CoV-2 was analyzed in TMPRSS2 expressing Vero6E cells. The experiments were independently performed twice in biological triplicate.

duplicate.

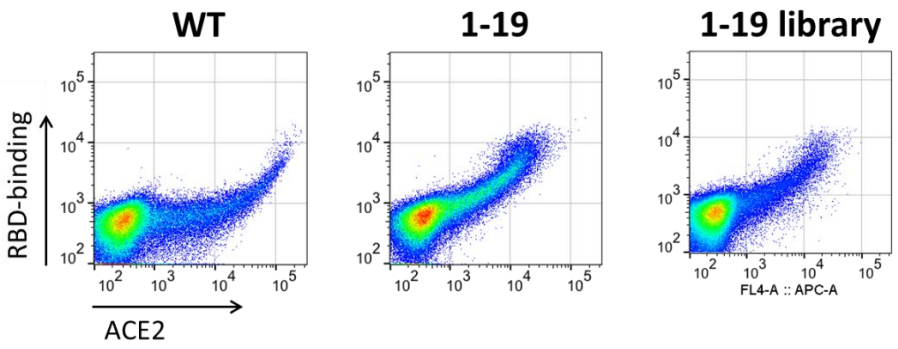

Figure S1. Second mutagenesis in 1-19 mutation that was one of the hits of first screening. The distribution of 1-19 library cells was relatively narrow and provided no better mutant than original 1-19 mutant in the individual validation.

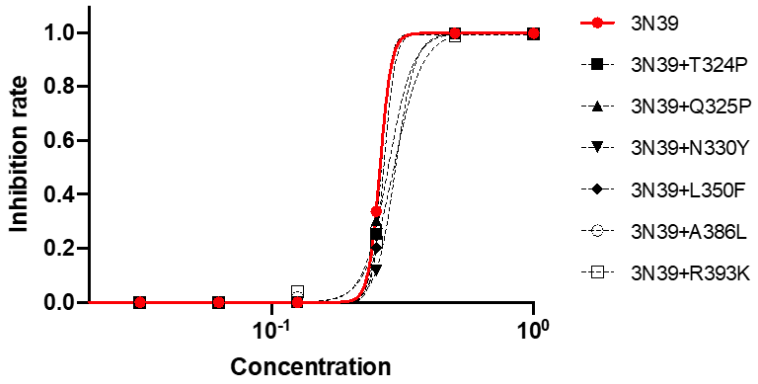

Figure S2. Additional PD2 mutation in 3N39 mutant. Induction of affinity-enhancing mutation in PD2 from Procko's paper failed to improve the capacity of the RBD neutralization. The experiments were independently performed twice and similar results were obtained. One representative data were shown.

a

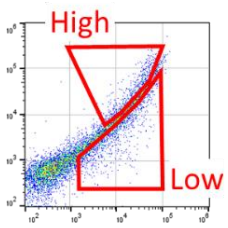
High
Low

b

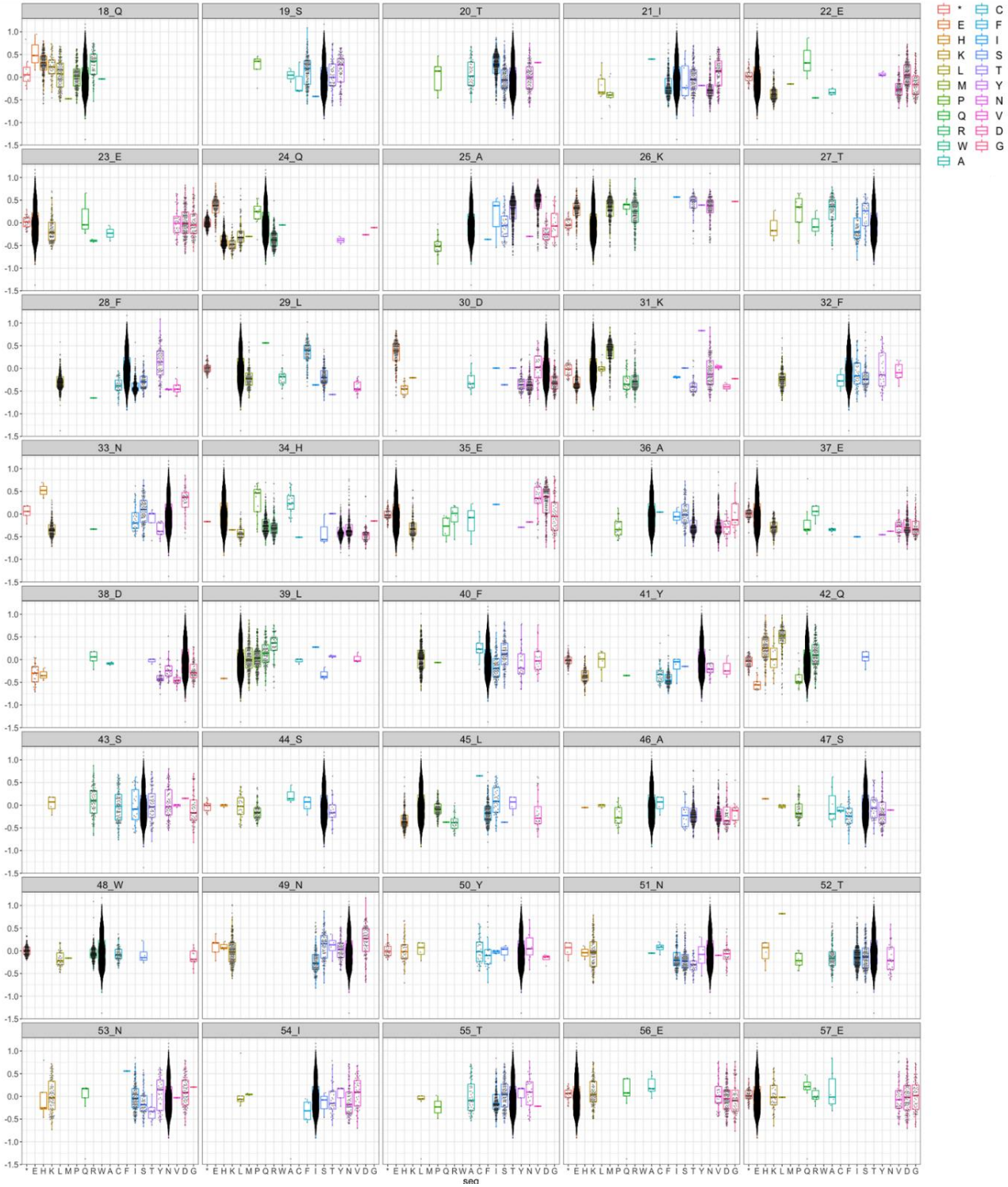
18_Q
19_S
20_T
21_I
22_E
23_E
24_Q
25_A
26_K
27_T
28_F
29_L
30_D
31_K
32_F
33_N
34_H
35_E
36_A
37_E
38_D
39_L
40_F
41_Y
42_Q
43_S
44_S
45_L
46_A
47_S
48_W
49_N
50_Y
51_N
52_T
53_N
54_I
55_T
56_E
57_E
1.0
0.5
0.0
-0.5
-1.0
-1.5
* E H K L M P Q R W A C F I S T Y N V D G
seq
* E H K L M P Q R W A C F I S T Y N V D G
* E H K L M P Q R W A C F I S T Y N V D G
* E H K L M P Q R W A C F I S T Y N V D G
* E H K L M P Q R W A C F I S T Y N V D G
* E H K L M P Q R W A C F I S T Y N V D G
C F I S T Y N V D G

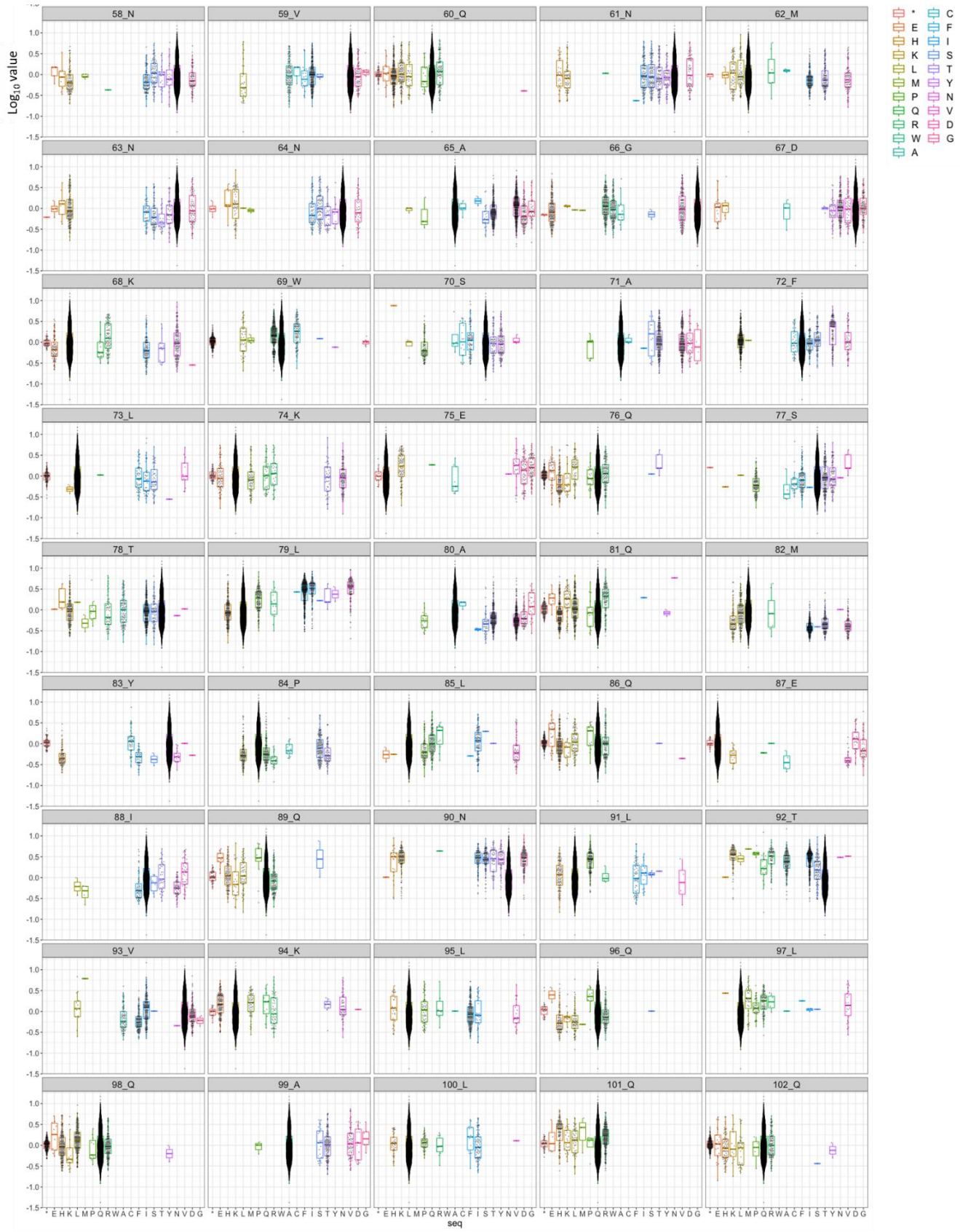
Log10 value
58_N
59_V
60_Q
61_N
62_M
63_N
64_N
65_A
66_G
67_D
68_K
69_W
70_S
71_A
72_F
73_L
74_K
75_E
76_Q
77_S
78_T
79_L
80_A
81_Q
82_M
83_Y
84_P
85_L
86_Q
87_E
88_I
89_Q
90_N
91_L
92_T
93_V
94_K
95_L
96_Q
97_L
98_Q
99_A
100_L
101_Q
102_Q
1.0
0.5
0.0
-0.5
-1.0
-1.5
* E H K L M P Q R W A C F I S T Y N V D G
seq
* E H K L M P Q R W A C F I S T Y N V D G

Figure S3. Sequence-to-affinity value in ACE2 residues 18-102 (PD1). (**a**) High and low affinity populations were sorted in first mutant library. (**b**) The affinity value of each mutant was defined as high/low read counts and plotted in each amino acid substitution. Mutants with multiple mutations were plotted in each mutation redundantly.

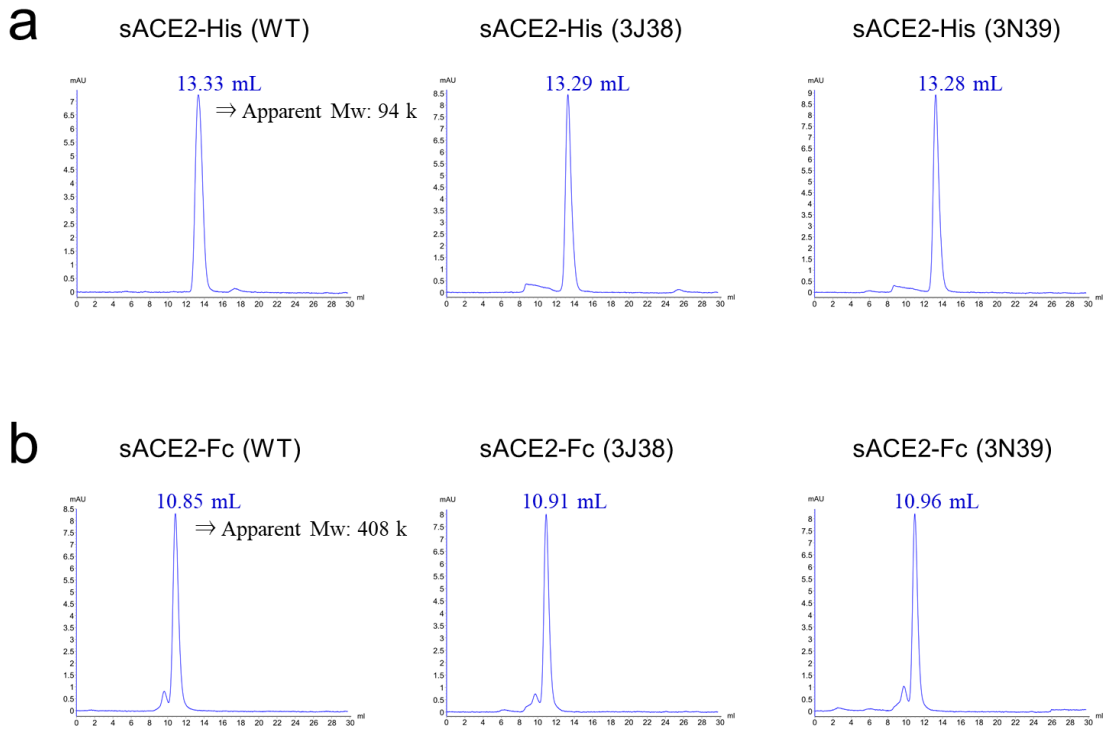

Figure S4. Analytical SEC of sACE2 proteins (**a**) Analytical SEC of His-tagged proteins used in analysis of surface plasmon resonance. (**b**) Analytical SEC of Fc-fused proteins used in to evaluate SARS-CoV-2 neutralizing activity.

	Sequence	Value
	20 30 40 50 60 70 80 90 100	
3N39	QSTIEEQVETFLDNFNHKAEDLFYQSSLASWNYNTNITEENVQNMNIAGDKWSAFLKEQSTFAQMYPLQEIQHLTVKLQLQALQQ	0.00
WT	QSTIEEQAKTFLDKFNHEAEDLFYQSSLASWNYNTNITEENVQNMNNAGDKWSAFLKEQSTLAQMYPLQEIQNLTVKLQLQALQQ	-7.24
1-19	QSIIEEQVMTFLDKFNHEAEDLFYQSSLASWKYNTNITEENVQNMNNAGDKWSAFLKEQSTLAQMYPLQEIQNLTVKLQLQALQQ	-2.13
1-19-37	QSIIEEQVMTFLDKFNHEAEDLFYQSSLASWKYNTNITEENVQNMNNAGDKWSAFLKEQSTLAQMYPLQEIQILTVKLQLQALQQ	-5.16
1-19-71	QSIIEEQVMTFLDKFNHEAEDLFYQSSLASWKYNTNITEENVQNMNNAGDKWSAFLKVQSTLAQMYPLQEIQNLAVKLQLQALQQ	-3.03
2-18	QSTIEEEVKTFLDLFNHEAEDLFYQSSLASWNYNTNITEENVQNMNNAGDKWSAFLKEQSSLAQMYPLQEIQTLTVKLQLQALQQ	-2.76
2-45	QSTIEEQAETFLDKFNHEAEDLFYQSSLASWNYNTNITEENVQNMNNAGDKWSAFLKEQSTLAQMYPLQEILNPTVKLQLQALQQ	-1.97
2-51	QSTIEDQVETFLDKFNHEAEDLFYQSSLASWNYNTNITEENVQNMNNAGDKWSAFLKEQSKLAQMYPLQEIQNPTVKLQLQALQQ	-1.78
2-53	HSTIEEQVETFLDKFNHEAEDLFYQSSLASWNYNTNITEENVQNMNNAGDKWSAFLKEQSTLAQMYPLQEIQNLAVMLQLQALQQ	-1.80
3J14	QYTIEDQVETFLDKFNHDAEDLFYQSSLASWIYNTNITEENVENMNNAGDKWSAFLKEQSTLALLYPLQEIQNLQVKLQLQALQQ	-0.92
3J38	KSTTEDQVETFLDKFNHDAEDLFYQSSLASWNYNTNITEENVQNMNNAGDKWSAFLKEQSTLALMYPLQEIQNLQVKLQLLALQQ	-0.85
3J45	QSIIEEQVKTFLEKFSHEAEDLFYQSSLASWNYNTNITEENVQNMNNAGDKWSAFLKEQSTLAQMYPLYEIQNLAVKLQLQALQQ	-2.36
3J80	QSTIEEQVETFLDKFNHEAEDLFYQSSLASWNYNTNITEENVQNMNNAGDEWSAFLKEQSSFAQMYPLQEIQNPTVKLQLQALQQ	-0.16
3J85	LSTIEEQAKTFLDKFNAEAEDLFYQSSLASWNYNTNITEENVQNMINAGDKWSAFLKEQSTLAQMYPLQEIQNLPVKLQLQALQQ	-0.01
3J89	QSTIEEQAKTFLDKFNREAEDLFYQSSLASWNYNTNITEENVQNMNNAGDKWSAFLKEQSTLAQMYPLQEIQDLSVKLQLEALQQ	-2.51
3J109	HSTIEEQVKTFLDMFNHEAEDLFYQSSLASWNYNTNITEENVQDMNNAGDKWFAFLKEQSTLAQMYPLQEIQDLTVKLQLQALQQ	-0.10
3J113	QSTIEEQAKTFLDMFNHKAEDLFYQSSLASWNYNTNITEENVRNMNNAGDKWFAFLKEQSTFAQMYPLQEIQDLTVKLQLQALQQ	0.06
3J120	QSTIEEEAKTFLDKFNHEAEDLFYQSSLASWNYNTNITEENVQNMNNAGDKWSAYLKERSALAQMYPLQEIQNLQVKLQLQALQQ	-0.75
3J121	KYTIEDQVETFLDKFNHEAEDLFYQSSLASWNYNTNITEENVQNMNIAGDKWSAFLKEQSTLAQMYPLQEIQNPTVKLQLQALQQ	-0.19
3J307	HSTTEDQVETFLDKFNHDAEDLFYQSSLASWNYNTNITEENVQYMNNAGDRWSAFLKEQTTFAQMYPLQEIQNLTVMLQLQALQR	-1.10
3J311	QSIIEEQAETFLDKFNHEAEDLFYQSSLASWNYNTNITEENVHNMNYAGDKWSTFLKEQSTVAQMYPLQEIQDLTVKLQLQALQP	-1.34
3J320	QSIIEEQVKTFLDKFNAEAEDLFYQSSLASWNYNTNITEENVQNMNNAGDKWSAFLKEQSRLAQMYPLQEIQNLQVKLQLQALHQ	0.06
3J323	QSTIEDQVETFLDKFNHDAEDLFYQSSLASWNYNTNITEENVQYMNNAGDKWSAFLKEQTALAQMYPLQEIQNLTVKLQLQALQQ	-0.59
3N27	QSTTEEQAETFLDMFNHEAEDLFYQSSLASWNYNTNITKENVQNMNNAGDKWSAFLKEQSTFAQMYPLQEIQDLTVKLQLQALQQ	-3.62
3N68	QSTIEEQAKTFLDKFNHEAEDLFYQSSLASWNYNTNITEEYVQNMNNAGDKWFAFLKEQSTLAQMYPLQEIQKLTVKLQLQALQQ	-5.07
3P4	QSIIEEQVMTFLDNFNHKAEDLFYQSSLASWNYNTNITEENVQNMNIAGDKWSAFLKEQSTFAQMYPLQEIQNLTVKLQLQALQQ	-0.10
3P8	QSTIEEQVETFLDNFNHKAEDLFYQSSLASWNYNTNITEENVLNMNNAWDKWFAFLKEQSSLAQMYPLQEIQNLQVKLQLQALQQ	-1.36

Table. S1 Amino acid sequence and RBD neutralization activity value of validated mutants.

The value of RBD neutralization activity was calculated as -log2 concentration of 50% RBD-sfGFP bound competing relative to 3N39.